

TEMPERATURE PROFILES AND WAVE STRUCTURES OBSERVED WITH IUVS/MAVEN STELLAR OCCULTATIONS.

H. Gröller, R. V. Yelle, T. Koskinen, *Lunar and Planetary Laboratory, University of Arizona, Tucson, AZ, USA (hgr@lpl.arizona.edu)*, **F. Montmessin, G. Lacombe**, *LATMOS, Université Versailles Saint-Quentin / CNRS, Guyancourt, France*, **S. Jain, J. Deighan, N. M. Schneider**, *Laboratory for Atmospheric and Space Physics, University of Colorado, Boulder, CO, USA*, **H. Nakagawa**, *Department of Geophysics, Tohoku University, Sendai, Miyagi, Japan*, **A. S. Medvedev**, *Max Planck Institute for Solar System Research, Göttingen, Germany*.

Introduction

We present the latest temperature profiles and wave/tides structures from stellar occultations observed by the Imaging Ultraviolet Spectrograph (IUVS) on the Mars Atmospheric and Volatile Evolution (MAVEN) Mission (Jakosky *et al.*, 2015).

Stellar occultation campaigns are executed over 5 successively orbits, targeting the same sequence of stars in each orbit. This results in a sequence of occultations at similar latitudes and local times but different longitudes. The IUVS instrument observes in the FUV and MUV channels covering the spectral range from 110 to 350 nm (McClintock *et al.*, 2014). Using both channels, complete temperature profiles from 30 to 150 km (10^1 to 10^{-6} Pa) are measured. The temperature profile for each occultation is calculated from the local density profile by applying the constraint of hydrostatic equilibrium to the CO₂ densities and using the algorithm described in Snowden *et al.* (2013). A detailed description of the retrieval process is given in Gröller *et al.* (2015) and Sandel *et al.* (2015).

Temperature Profiles and Wave Structures

Temperature profiles, targeting η UMa over 5 successively orbits during campaign 3 and κ Sco during campaign 5 are shown in Figure 1, in the top and the bottom row, respectively. The left panel shows the retrieved temperature profiles including their uncertainties (solid colored lines) and the mean value (orange solid line) with the root sum square of the errors for the individual temperature profiles (orange shaded area). The colored dash-dotted lines represent the Mars Climate Database (MCD) predicted profiles for the same geometries (latitude, longitude, local time and L_S) as the occultations. The MCD is a collection of model predictions using the LMD-GCM (González-Galindo *et al.*, 2009). An overview of the Mars Climate Database can be found in Millour *et al.* (2014). In the top left panel, the measured temperature profiles are in agreement with the MCD profiles for pressure lower than 1 Pa (around 30 km), however, more wave and/or tides structures are present in the measured profiles. The black dash-dotted line indicates the CO₂ saturation temperature.

At a pressure level of 10^{-2} Pa (around 90 km altitude) the retrieved temperatures reaches the saturation temperature which is an indication for cloud formation. The bottom left panel shows the comparison for κ Sco. The MCD temperature profiles are in agreement up to a pressure of 10^{-3} Pa (around 110 km altitude). Both sets of temperature profiles show similar wave structures but with different phases. At lower pressures (higher altitudes) the IUVS temperature profiles are up to 40 K colder than MCD temperatures.

Different possibilities are mentioned in the literature to explain the decrease in temperature at lower pressures ($10^{-3} - 10^{-4}$ Pa) as seen in most of the temperature profiles of Figure 1. McDunn *et al.* (2010) suggest that the radiative cooling rates in the atmosphere may be larger than that contained in the models causing the lower atmosphere to cool faster. An enhanced CO₂ 15 μ m cooling due to elevated O densities together with gravity wave-induced cooling leads to temperature decreases of ~ 5 to ~ 20 K (equatorial to high altitudes) is mentioned in Medvedev *et al.* (2015).

The three panels in the middle of the figure show three different ways of illustrating the presence of waves and/or tides. The left panel of those three shows the difference between the mean temperature profile and a 3rd degree polynomial fit of the mean profile. The middle panel shows the difference for each single occultation and the mean temperature profile.

The fourth panel illustrates the wave structure for each occultation by taking the difference between the 3rd degree polynomial fit of the mean temperature profile and each occultation. The right most panel shows the difference between the environmental lapse rate and the dry adiabatic,

$$\Delta\Gamma(T, r) = \Gamma_{env}(T, r) - \Gamma_{dry\ adiab}(T, r). \quad (1)$$

The environmental lapse rate Γ_{env} is the negative temperature gradient,

$$\Gamma_{env}(T, r) = -\frac{dT}{dr} \quad (2)$$

and the dry adiabatic lapse rate $\Gamma_{dry\ adiab}$ is calculated by

$$\Gamma_{dry\ adiab}(T, r) = \frac{g(r)}{c_p(T, r)} \quad (3)$$

REFERENCES

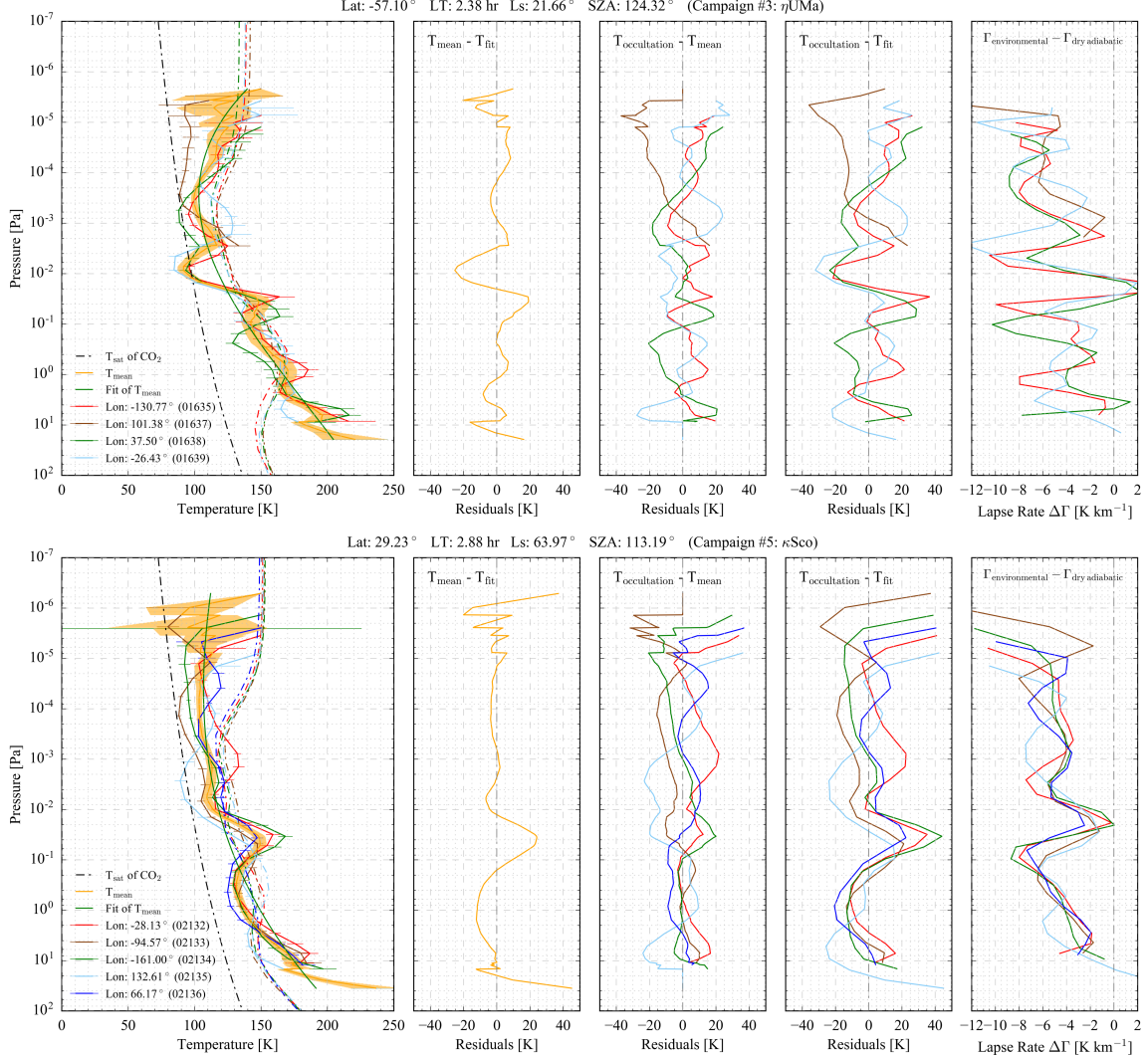


Figure 1: Longitude variability of the temperature profiles for three different cases.

with the altitude r dependent gravity g and the temperature T and altitude r dependent specific heat capacity $c_p(T, r)$. In case of Mars where the CO₂ abundance is more than two orders of magnitudes higher than the O abundance for altitudes lower than 150 km one can use the specific heat capacity for CO₂,

$$c_{p,\text{CO}_2}(T, r) = 7.4131 \times 10^6 + 1.0182 \times 10^4 (T - 200) \quad (4)$$

instead of

$$c_p = \frac{n_{\text{CO}_2} c_{p,\text{CO}_2} + n_{\text{O}} * c_{p,\text{O}}}{n_{\text{CO}_2} + n_{\text{O}}} \quad (5)$$

if the density of O is comparable to CO₂. The environmental lapse rate in the top row exceeds the dry adiabatic which is an indication for a wave braking at a pressure

level around 6×10^{-2} Pa, which equals an altitude of around 90 km.

Acknowledgements

This work was supported by NASA as part of the MAVEN Mission.

References

- González-Galindo, F., Forget, F., López-Valverde, M. A., Angelats i Coll, M., Millour, E. (2009), A ground-to-exosphere martian general circulation model: 1.

REFERENCES

- Seasonal, diurnal, and solar cycle variation of thermospheric temperatures, *Journal of Geophysical Research*, 114, E04,001.
- Gröller, H., R. V. Yelle, T. T. Koskinen, F. Montmessin, G. Lacombe, N. M. Schneider, J. Deighan, A. I. F. Stewart, S. K. Jain, M. S. Chaffin, M. M. J. Crismani, A. Stiepen, F. Lefèvre, W. E. McClintock, J. T. Clarke, G. M. Holsclaw, P. R. Mahaffy, S. W. Bouger, and B. M. Jakosky (2015), Probing the Martian atmosphere with MAVEN/IUVS stellar occultations, *Geophysical Research Letters*, 42(21), 9064–9070.
- Jakosky, B. M., R. P. Lin, J. M. Grebowsky, J. G. Luhmann, D. F. Mitchell, G. Beutelschies, T. Priser, M. Acuna, L. Andersson, D. Baird, D. Baker, R. Bartlett, M. Benna, S. W. Bouger, D. Brain, D. Carson, S. Cauffman, P. Chamberlin, J.-Y. Chaufray, O. Cheatom, J. T. Clarke, J. Connerney, T. Cravens, D. Curtis, G. Delory, S. Demcak, A. De-Wolfe, F. Eparvier, R. Ergun, A. Eriksson, J. Espley, X. Fang, D. Folta, J. L. Fox, C. Gomez-Rosa, S. Habenicht, J. Halekas, G. Holsclaw, M. Houghton, R. Howard, M. Jarosz, N. Jedrich, M. Johnson, W. Kasprzak, M. Kelley, T. King, M. Lankton, D. Larson, F. Leblanc, F. Lefèvre, R. Lillis, P. Mahaffy, C. Mazelle, W. E. McClintock, J. McFadden, D. L. Mitchell, F. Montmessin, J. Morrissey, W. Peterson, W. Possel, J. A. Sauvaud, N. Schneider, W. Sidney, S. Sparacino, A. I. F. Stewart, R. Tolson, D. Toublanc, C. Waters, T. Woods, R. V. Yelle, and R. W. Zurek (2015), The Mars Atmosphere and Volatile Evolution (MAVEN) Mission, *Space Science Reviews*, 195(1-4), 21–48.
- McClintock, W. E., N. M. Schneider, G. M. Holsclaw, J. T. Clarke, A. C. Hoskins, I. Stewart, F. Montmessin, R. V. Yelle, and J. Deighan (2014), The Imaging Ultraviolet Spectrograph (IUVS) for the MAVEN Mission, *Space Science Reviews*, 1–50.
- McDunn, T. L., S. W. Bouger, J. Murphy, M. D. Smith, F. Forget, J.-L. Bertaux, and F. Montmessin (2010), Simulating the density and thermal structure of the middle atmosphere ($\sim 80 - 130$ km) of Mars using the MGCM-MTGCM: A comparison with MEX/SPICAM observations, *Icarus*, 206(1), 5–17.
- Medvedev, A. S., F. González-Galindo, E. Yiğit, A. G. Feofilov, F. Forget, and P. Hartogh (2015), Cooling of the Martian thermosphere by CO₂ radiation and gravity waves: An intercomparison study with two general circulation models, *Journal of Geophysical Research: Planets*, 120(5), 913–927.
- Millour, E., F. Forget, A. Spiga, T. Navarro, J. B. Madeleine, A. Pottier, L. Montabone, L. Kerber, A. Colaitis, F. Lefèvre, F. Montmessin, J. Y. Chaufray, M. A. López Valverde, F. González-Galindo, S. R. Lewis, P. L. Read, M. C. Desjean, J. P. Huot, and M. G. D. Team (2014), A new Mars Climate Database v5.1, *The Fifth International Workshop on the Mars Atmosphere: Modelling and Observation*, p. 1301.
- Sandel, B. R., H. Gröller, R. V. Yelle, T. T. Koskinen, N. K. Lewis, J.-L. Bertaux, F. Montmessin, and E. Quémérais (2015), Altitude profiles of O₂ on Mars from SPICAM stellar occultations, *Icarus*, 252, 154–160.
- Snowden, D., R. V. Yelle, J. Cui, J. E. Wahlund, N. J. T. Edberg, and K. Ågren (2013), The thermal structure of Titan's upper atmosphere, I: Temperature profiles from Cassini INMS observations, *Icarus*, 226(1), 552–582.